AD-A071 508 CALIFORNIA INST OF TECH PASADENA SEISMOLOGICAL LAB F/G 8/7
SHOCK EFFECTS IN CARBONATES.(U)
FEB 77 J VIZGIRDA, T J AHRENS DNA001-76-C-0218

UNCLASSIFIED CIT-SL-SWL-1 DNA-4715Z NL

1 OF 1
AD
A071508

END
DATE
FILMED
8-79
DDC

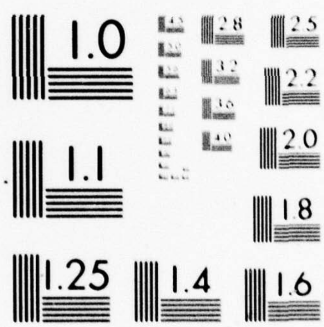

MICROCOPY RESOLUTION TEST CHART
NATIONAL BUREAU OF STANDARDS-1963-A

DNA 4715Z

SHOCK EFFECTS IN CARBONATES

Joana Vizgirda
Thomas J. Ahrens

California Institute of Technology
Seismological Laboratory
Division of Geological and
Planetary Sciences
Pasadena, California 91125

28 February 1977

Interim Report for Period 1 March 1976—28 February 1977

CONTRACT No. DNA 001-76-C-0218

APPROVED FOR PUBLIC RELEASE;
DISTRIBUTION UNLIMITED.

THIS WORK SPONSORED BY THE DEFENSE NUCLEAR AGENCY
UNDER RDT&E RMSS CODE B34407T464 Y99QAXSA00189 H2590D.

Prepared for
Director
DEFENSE NUCLEAR AGENCY
Washington, D. C. 20305

UNCLASSIFIED

SECURITY CLASSIFICATION OF THIS PAGE (When Data Entered)

REPORT DOCUMENTATION PAGE

READ INSTRUCTIONS BEFORE COMPLETING FORM

1. REPORT NUMBER: DNA 4715Z	2. GOVT ACCESSION NO. / 3. RECIPIENT'S CATALOG NUMBER
4. TITLE (and Subtitle): SHOCK EFFECTS IN CARBONATES	5. TYPE OF REPORT & PERIOD COVERED: Interim Report for Period 1 Mar 76– 28 Feb 77
	6. PERFORMING ORG. REPORT NUMBER: CIT-SL-SWL-1
7. AUTHOR(s): Joana Vizgirda and Thomas J. Ahrens	8. CONTRACT OR GRANT NUMBER(s): DNA 001-76-C-0218
9. PERFORMING ORGANIZATION NAME AND ADDRESS: California Institute of Technology, Seismological Laboratory, Division of Geological and Planetary Sciences, Pasadena, California 91125	10. PROGRAM ELEMENT, PROJECT, TASK AREA & WORK UNIT NUMBERS: Subtask Y99QAXSA001-89
11. CONTROLLING OFFICE NAME AND ADDRESS: Director, Defense Nuclear Agency, Washington, D.C. 20305	12. REPORT DATE: 28 February 1977
	13. NUMBER OF PAGES: 22
14. MONITORING AGENCY NAME & ADDRESS (if different from Controlling Office)	15. SECURITY CLASS (of this report): UNCLASSIFIED
	15a. DECLASSIFICATION/DOWNGRADING SCHEDULE

16. DISTRIBUTION STATEMENT (of this Report)

Approved for public release; distribution unlimited.

17. DISTRIBUTION STATEMENT (of the abstract entered in Block 20, if different from Report)

18. SUPPLEMENTARY NOTES

This work sponsored by the Defense Nuclear Agency under RDT&E RMSS Code B34407T464 Y99QAXSA00189 H2590D.

19. KEY WORDS (Continue on reverse side if necessary and identify by block number)

Eniwetok
Pacific Test Site
Shock Waves
Cratering
Peak Pressures

20. ABSTRACT (Continue on reverse side if necessary and identify by block number)

Permanent deformation of very small crystallites of carbonate minerals, such as those occurring in the Eniwetok core, has been examined using the following techniques: (a) Peak broadening of X-ray powder diffractometer patterns due to decreasing effective grain size with increasing shock deformation is observed. This effect is clearly seen in the core material taken from directly under the Cactus explosion. (b) Angular strain in calcite single crystals has been observed in Debye-Scherrer patterns of laboratory shocked samples and single-

(over)

DD FORM 1473, 1 JAN 73 EDITION OF 1 NOV 65 IS OBSOLETE

UNCLASSIFIED

SECURITY CLASSIFICATION OF THIS PAGE (When Data Entered)

20. ABSTRACT (Continued)

crystallites from the Eniwetok core. Tentative peak shock pressures of ~8 kbar at a depth of ~15 m decaying to ~3 kbar at a depth of ~30 m are inferred on the basis of very preliminary data. (c) Shock-induced erasure of defect spectra, as examined by electron-spin resonance (ESR) techniques, is observed in carbonate material, both shocked in the laboratory and by the Cactus explosion. This effect is yet "uncalibrated." (d) Also using the ESR techniques, a systematic loss of fine structure of the resonance of Mn^{++} impurities in calcite is observed with increasing shock pressure, both in laboratory shocked samples and those in the Cactus core.

approximately

Mn(++)

PREFACE

We appreciate the encouragement and help of Jerry Stockton (RDA), David Roddy (USGS), and F. Tsay (JPL) have given us in this work. The introduction to the problem area presented to us by Captains B. Ristvet and W. Ullrich of AFWL, and the superb X-ray diffraction work carried out under Captain Robert Couch, McClellan AFB were important to achieving many of the results summarized in this report.

TABLE OF CONTENTS

	Page
PREFACE	1
INTRODUCTION	3
RESEARCH SUMMARY	4
Angular Strain Analysis	4
Particle Size Analysis	7
Shock-Induced Erasure of Radiation Damage Centers	8
Lattice Distortion Effects-Evidence From Mn^{++}	10
CONCLUSION	13
REFERENCES	15

INTRODUCTION

During the previous year, we have both developed quantitative criteria for determining the peak shock stresses experienced by carbonate rocks, and applied these to infer the peak shock pressure history of carbonate core (XC-1) materials recovered from ground zero beneath the Cactus explosion crater at Eniwetok. Our efforts were directed toward three simultaneously conducted research phases: a) the development of quantitative methods of shock effect analyses, b) careful application of these methods to Cactus core material, and c) comparison of Cactus core results with analagous carbonate rocks experimentally shocked in the laboratory to known stress levels.

The first of these phases demanded the greatest expenditure of effort, and the techniques that have been developed are still in a process of refinement. Due to the nature of the core material, an inhomogeneous, very fine-grained biogenic carbonate, traditional optical methods of shock effect documentation have, to date, proved to be unproductive. Application of X-ray and electron spin resonance techniques was subsequently attempted; the resulting data appear to be quantitatively relatable to the stress levels imposed on carbonate rocks. Debye-Scherrer arc spreading, X-ray diffraction peak broadening, radiation damage erasure, and electron spin resonance (ESR) Mn^{++} zero-crystal-field splitting effects are all observed to vary consistently with depth within the XC-1 core section. An additional, and very fortunate property of all the above mentioned effects is their first-order independence of the relative abundance of the carbonate polymorphs, aragonite and calcite, found in these rocks. Analogous variations are observed in experimentally shocked specimens of both single-crystal calcite and Eniwetok material sampled from areas unaffected by the Cactus event. Comparing data from in-situ and laboratory recovered carbonates has enabled us to place upper and lower limits on the stresses experienced at various levels in the XC-1 core.

In addition to the already mentioned refinement of shock-effect detection methods, further recovery experiments should allow us to more narrowly limit shock pressures. Also, physical models providing a theoretical basis for the processes which take place upon shock processing fine-grained carbonates are presently under development. This understanding would be of considerable value in predicting the response of shocked carbonate materials occurring in other geologies. In the case of the electron spin resonance method, the work on the Cactus core material is, in fact, a pioneering effort in this area of research. It is likely that the results of this research program can be applied to other explosively shocked and meteorite impacted rocks.

RESEARCH SUMMARY

Angular Strain Analysis

A systematic increase in angular strain with pressure, analagous to that measured in laboratory shocked specimens, is displayed by calcite crystals isolated from XC-1 core material. (see Table 1.) Experimental single crystal calcite data provide a preliminary calibration curve relating observed strain to a documented shock pressure (Figure 1). In addition to such an empirical correlation, a theoretical model based on compressional data of Ahrens and Gregson (1964) has been applied to the material. Knowing the pressure-volume behavior of a mineral, shock pressure may be explicitly related to angular strain, θ_m, by the following relation

$$\theta_m = \tan^{-1}\left[\sqrt{\frac{V_o}{V}}\right] - \tan^{-1}\left[\sqrt{\frac{V}{V_o}}\right] \qquad (1)$$

V_o and V represent initial and compressed volumes, respectively. Equation (1) is applicable in the region of deformational behavior at pressures not exceeding those of a shock-induced phase change which, in calcite, occurs at ~16-17 kbar (Ahrens and Gregson, 1964). According to this model, it is inferred that calcite from a depth of 41.8' to 43' has been exposed to peak pressures of approximately 10 ± 5 kbars. Calcite from depths of ~90' indicates strains corresponding to less than ~5 kbars.

As first observed by R. Couch, aragonite displays a more consistent variation of Debye-Scherrer pattern angular broadening with depth, i.e., shock deformation, than does calcite. However, an extensive series of shock recovery experiments on single crystal aragonite, followed by Debye-Scherrer investigations of these samples, will be required before an observed-angular-strain to impact-stress relationship can be quantified. We propose to do just this in the future. A comparison of calculated stress levels from angular strain in both aragonite and calcite would serve to verify and more narrowly limit the shock pressure inferred for same depth in the core. Toward this end, preliminary equation of state data for aragonite has been obtained during the present project.

TABLE 1

Ni-K_α Debye-Scherrer Reflection Strain Angles[a)]

A. CIT Shocked Calcite[b)], Single Crystal (101)

Diffraction Line Arc (°), Rhombic Notation

Shock Pressure (kbar)	(102)	(100)	(113)	(202)	(204)	(208)
0.0[c)]	0.00 ±.05	0.00 ±0.04	0.00 ±0.10	0.00 ±0.13	0.00 ±0.093	0.00 ±0.11
7	0.25 ±0.21	0.46 ±0.30	0.26 ±0.19	0.68 ±0.20	0.17 ±0.17	0.23 ±0.25
36	1.23 ±0.63	2.23 ±1.37	1.76 ±1.06	1.81 ±0.89	1.27 ±1.09	1.55 ±0.90

B. Calcite Crystals from Cactus, XC-1 Core Hole

Diffraction Line Arc (°), Rhombic Notation

Core Interval (feet)	(102)	(100)	(113)	(202)	(204)	(200)
41.4-48	0.38* ±0.18	1.03 ±0.97	0.20 ±0.27	0.46 ±0.47	0.29 ±0.20	0.17 ±0.18
83-87	0.30* ±0.11	0.19 ±0.18	0.38 ±1.22	0.22* ±0.09	0.24* ±0.16	0.26* ±0.03
87-91	0.25* ±0.06	0.31 ±0.43	0.02 ±0.15	0.17 ±0.16	0.16 ±0.15	0.15 ±0.15

a) X-ray diffraction patterns taken by R. Couch.
b) Samples supplied by F. Hörz.
c) Sample, AFWL Standard calcite #6, unshocked sample gave 0.04 to 0.11°, natural beam width. The natural beam width has been subtracted from data for each diffraction peak.
* Lowest uncertainty, angular strain data.

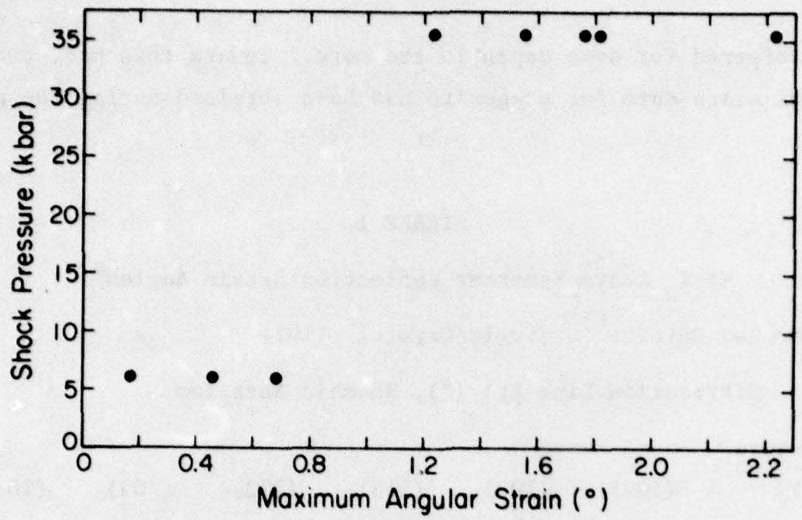

Figure 1. Maximum angular strain vs. pressure in shock recovered calcite.

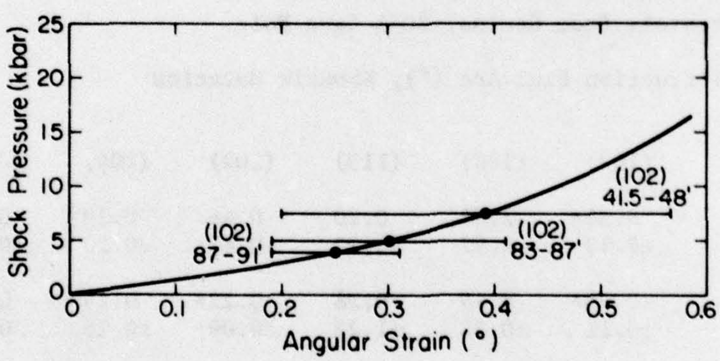

Figure 2. Preliminary shock pressure vs. angular strain based on Equation (1). Data plotted are for (102) calcite reflection.

Particle Size Analysis

Powder X-ray diffraction spectra of XC-1 core material display a systematic decrease in broadening of both calcite and aragonite peaks, measured at half their maximum intensity, with increasing depth of sample. Tracings were obtained with a standard 45 Kv-Cu X-ray goniometer; unstrained, biogenic calcite was used as a reference standard. Diffraction peak broadening is known to be related to the mean dimension, D, of the crystallites composing the powder according to the following equation from Klug and Alexander, p. 491:

$$D = \frac{K\lambda}{\beta\cos\theta} \qquad (2)$$

K is a constant related to the crystallite shape, λ is the wave length of the X-rays, θ the Bragg reflection angle for the (102) calcite peak, and β the half-width of that peak at half-maximum intensity.

The variation in crystallite size with depth in the XC-1 Cactus core is plotted in Figure 3. Although data points from intermediate to lower core samples show considerable scatter, those from the uppermost levels are significantly displaced toward the fine end of the granulation scale. Comparison with recovery data indicates that the shallow XC-1 material was exposed to pressures in excess of 2 kbars. Successful recoveries of saturated core material shocked to ~20 kbars have been achieved, but X-ray diffraction data on these samples is not yet available.

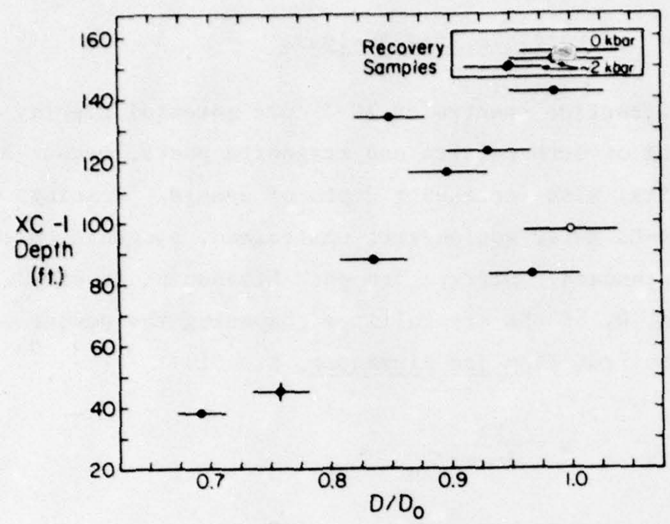

Figure 3. Variation of mean crystallite dimension, D, relative to that of unstrained biogenic calcite, D_0, as inferred from calcite (102) peak broadening. Preliminary data for grain sizes in two shock-recovered water-saturated cores (10' depth, XRU-3) and a control sample (0.0 kbar) are also indicated.

Shock-Induced Erasure of Radiation Damage Centers

The electron spin resonance peak attributed to intracrystalline radiation damage displays a unique pattern in spectra of laboratory and Cactus explosion shocked specimens. Natural U^{238}, K^{40}, and cosmic ray influences are believed to produce vacancies in the $CO_3^{=}$ sites of both aragonite and calcite; the observed spectral peak is presumably due to the resonance of free electrons occupying these vacancies. Comparison of unshocked and laboratory shocked (2→17 kbars) carbonates indicates that the intensity of this feature consistently decays with the application of increasing stresses. It is hypothesized that shocked induced annealing provides the erasure mechanism. Figure 4 depicts the variation in radiation damage peak with depth in the XC-1 Cactus core. As seen in this diagram, heating the specimens to 430°C somewhat decreases the amplitude of this feature. However, the depth vs. intensity pattern remains unaltered and shock rather than thermal erasure is concluded to be the dominant mechanism. A detailed series of chemical analyses would be required to accurately calibrate this effect in terms of applied shock stress. Of interest is the high level of

ESR radiation damage observed in the 36.5' (approximately the fall-back breccia-in-situ rock interface level). This radiation damage is unaffected by heating to 430°C and is considerably greater than seen in any of the other core material. This material may have experienced high fluxes of gammas and low-energy neutrons. On a simplistic level, the total radiation dose of this material may be calibratable. That this is so, is suggested by a preliminary experiment in which a Co^{60} source was used to irradiate Iceland spar with a dose of 1.2×10^6 rads (Figure 5G) and annealing at 600°C for 20 min., Figure 5H.

We thus, tentatively, interpret the amplitude of the relative damage ESR spectrum versus depth (Figure 4) as resulting from two competing effects as follows: the non-thermal or non-shock eraseable peak in the uppermost core appears to be radiatively induced by the device...this effect decays to a negligible value at a depth of between 46' to 89' below which the shock wave appears to have attenuated the natural radiative damage spectral resonance peak, the latter effect decreasing with depth.

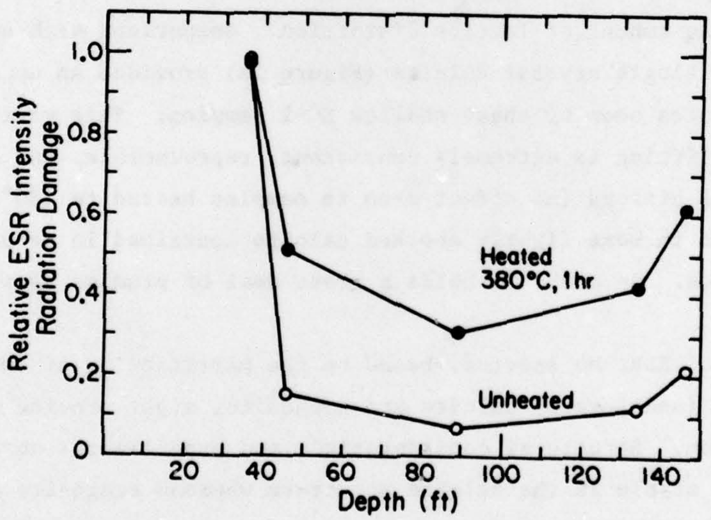

Figure 4. Relative intensity of radiation-damage ESR peak at ~3300 Gauss at 9.1 GHz versus depth for XC-1 core, from Cactus crater unheated and heated to 430°C for one hour. Two effects are superimposed. At shallow depth, the non-erasable device-induced radiation damage dominates, whereas between ~90 to ~145 ft. the natural radiation damage is progressively less-erased as the result of the decaying shock wave.

Lattice Distortion Effects-Evidence From Mn^{++}

The sensitivity of the ESR method to paramagnetic elements allows for the detection of both the presence and structural positioning of Mn^{++}, a common trace constituent of carbonates, substituting for Ca^{++} in the crystal lattice. In an undistorted octahedral environment (6 oxygen anions surrounding a Mn^{++} ion) provided by the calcite structure, the $3d^5$ electrons of Mn^{++} assume an energetically favorable configuration known in crystal field theory as "zero-field" splitting. This "energy distribution" appears in the ESR Mn^{++} spectra as a distinctive doublet feature (9.1 GHz resonance at ∿3540 Gauss) corresponding to the transition $I = 5/2$, $S = +1/2 \rightarrow S = -1/2$. A severe change in the ligand field and/or disturbance of host lattice structure appears to introduce a five-fold electron spin degeneracy which is reflected in the ESR spectra (∿3540 Gauss) as a single peak. A consistent increase in the amount of splitting, and hence, decreasing shock deformation with depth is observed for XC-1 core samples (Figures 5 & 6). In particular, samples from depths of 36.5 and 41.4→48.1 feet indicate a considerable amount of lattice distortion. Comparison with spectra of laboratory shocked single crystal calcite (Figure 5A) provides an upper limit of 55 kbars for pressures seen by these shallow XC-1 samples. This variation in Mn^{++} zero-field splitting is extremely consistent, reproducible, and apparently independent of thermal history (no effect seen in samples heated to 430°C). It has also been observed in some lightly shocked calcite contained in several carbonaceous meteorites. As such, it holds a great deal of promise as a stress level indicator.

Another feature of ESR, Mn spectra, based on the partitioning of two Mn oxidation states between (undeformed) calcite and aragonite, might provide a means of pressure calibration. Structural considerations and experimental observations indicate that Mn^{++} is stable in the calcite structure whereas aragonite accommodates Mn^{+++} (Low & Zeira, 1972). However, shocking the aragonite possibly affects its crystal lattice so that it can no longer provide a stable configuration for Mn^{+++} (Gibbons, Ahrens & Rossman, 1974). Under such deforming conditions and in the presence of a reducing ionic species (abundant in an aqueous environment) Mn^{+++} is reduced to Mn^{++}. Since the partitioning of these two states is effectively complete and the temperature contribution to the reducing transition apparently minimal, only Mn^{++} detected in aragonite might be explained as a shock pressure effect. Such an effect is very tentatively indicated by analyses of core material experimentally shocked in the 2→17 kbar range. However, its variation is not consistent and numerical shock pressures cannot at this time be inferred from the data. The consistency may be observed by widely varying Mn content (unknown) and aragonite-calcite ratios (aragonite content varies erratically from 0→94% in the XC-1 core); further chemical analyses will be required before the validity of this method can be established.

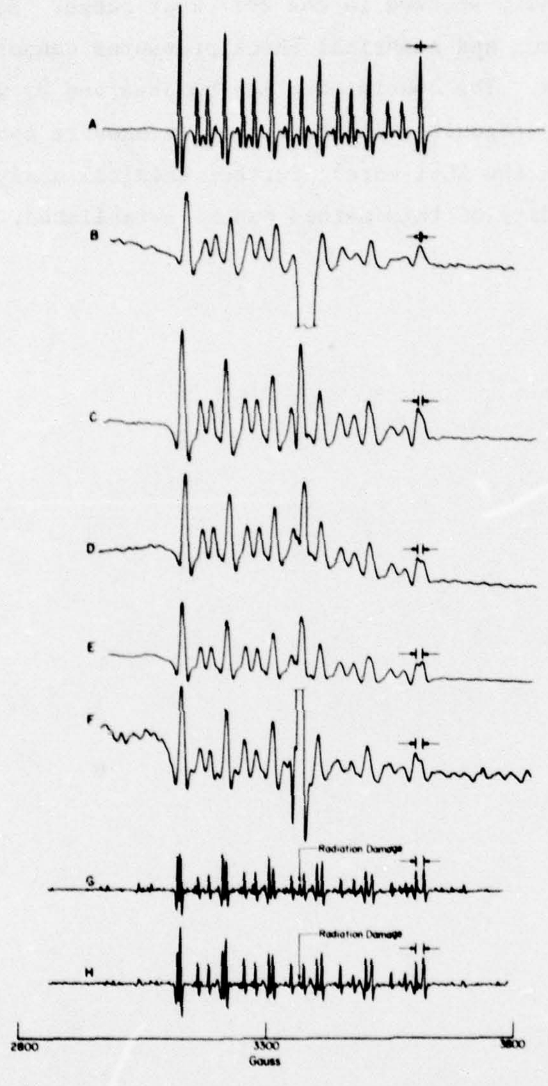

Figure 5. ESR spectra taken at 9.1 GHz. Splitting of ~3540 Gauss peak is indicated above the right hand side of each spectrum. A = Shot #117, pure calcite shocked to 55 kbar. Note complete absence of 3540 Gauss split peak. B = spectra of most intensely shocked Cactus sample from a depth of 36.5 ft., XC-1. Note absence of 3540 Gauss split peak. C = 41.4-48.1 ft., XC-1. D = 87-91 ft., XC-1. E = 133-135 ft., XC-1. F = 146 ft., XC-1. G = pure calcite unshocked; notice very wide doublet in spectra at 3540 Gauss and radiation-induced damage peak ~3300 Gauss produced by exposure to 1.2 x 10^6 rads of Co^{60} radiation. H = same sample as in G, except radiation-induced damage peak partially annealed by application 600°C for 20 min.

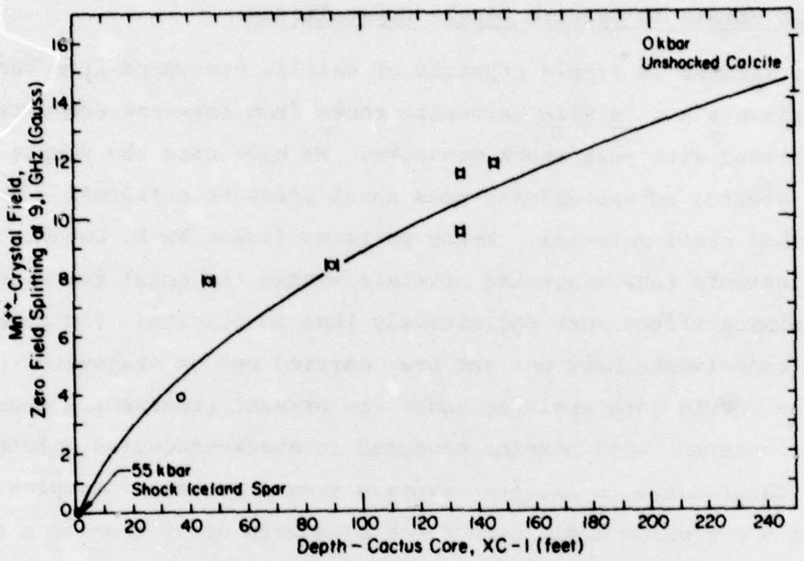

Figure 6. Magnitude of "zero-field" splitting of ∿3540 Gauss peak versus depth. Magnitude of splitting of 55 kbar shocked calcite and unshocked calcite shown for conceptual purposes only.

CONCLUSION

It appears possible, by examining non-elastic permanent deformations of very small crystallites of carbonate minerals, such as occur in the Eniwetok cores, to relate these deformations via possibly four different shock effects, to peak shock pressure and appropriate equations of state. The techniques which appear applicable, and in some cases, have already tentatively been applied to determining peak shock pressures for aliquots of core taken directly beneath the Cactus explosion (Eniwetok) are:

(1) Peak Broadening in X-Ray Powder Diffractometer Spectra.

We have observed a systematic decrease of the effective size of the average diffracting crystallites of calcite and aragonite for successively more intensely shocked in-situ coral material. Samples recovered from ∿2 kbar stress levels, indicate a slight decrease in crystallite size similar to that observed in the rock at depths of ∿50 m at the Cactus site. Detailed analysis of aliquots of initially unshocked coral, shocked in the laboratory has not yet been carried out.

(2) Angular Strain in Calcite Single Crystallites.

The angular strains in single crystals of calcite recovered from both laboratory experiments and in-situ carbonate rocks from Eniwetok demonstrate a systematic increase with peak shock pressure. We have used the single crystal data to provide an approximate peak shock pressure calibration for the in-situ shocked coral material. X-ray patterns (taken by R. Couch, McClellan AFB) indicate that aragonite crystals within the coral demonstrate the angular straining effect more definitively than in calcite. The appropriate calibration experiments have not yet been carried out on aragonite.

Although the strain data analyzed under the present program are scanty, they are not inconsistent with strains measured in shock-recovered calcite. Angular strain measurements in calcite crystals from a series of samples from beneath the Cactus explosion imply peak shock pressures of $\sim$8 kbar at a depth of $\sim$15 m decaying to $\sim$3 kbar at a depth of $\sim$30 m. These values are, at present, tentative. We expect upon examination of shock deformation in aragonite to obtain a better grasp on the shock-wave amplitudes.

(3) Shock-Induced Erasure of Defect Spectra in Calcite.

Electron-spin resonance spectra for a series of aliquotes of shocked carbonate material, both shocked in the laboratory and by the Cactus explosion, demonstrate the major feature observed is the resonance of an electron in a $CO_3^{=}$ vacancy. This feature which is presumed to arise from the natural radiogenic sources is apparently very sensitive to the stress history of calcite. A systematic decrease in amplitude of this resonance, which occurs at $\sim$3300 Gauss and 9.1 GHz, is observed to occur for material shocked in the laboratory over the range 2 to 17 kbar. A similar change in spectra is observed in samples explosively shocked, in-situ. A detailed series of measurements to "calibrate" this effect in terms of strain, and ultimately, shock stress, has not yet been carried out.

(4) Effect of Shock on Zero-Field Splitting of Mn^{++} in Calcite.

Recently we discovered a systematic loss of fine structure in electron spin resonance spectrum arising from Mn^{++}, substituting for Ca^{++} in calcite for samples exposed to increasing amplitude shock waves in the 2 to 38 kbar range. A similar variation with depth, and hence, effectively shock pressure, is observed in shocked coral from Eniwetok and also in some lightly shocked calcite in several meteorites.

REFERENCES

Ahrens, T. J., and V. G. Gregson, 1964. Shock compression of crustal rocks: data for quartz, calcite and plagioclase rocks, J. Geophys. Res., 69, 4839-4874.

Ahrens, T. J., and R. K. Linde, 1968. Response of brittle solids to shock compression, in Behavior of Dense Media Under High Dynamic Pressures, Proc. Symposium High Dynamic Pressure, Paris, 1967, Gordon and Breach, New York, pp. 325-336.

Gibbons, R. V., T. J. Ahrens and G. R. Rossman, 1974. A spectroscopic interpretation of the shock-produced color change in Rhodonite ($MnSiO_3$): The shock-induced reduction of MnIII to MnII, American Mineralogist, 59, 177-182.

Klug, H. P., and L. E. Alexander, 1954. X-ray Diffraction Procedures, John Wiley, New York.

Low, W., and S. Zeira, 1972. ESR spectra of Mn^{2+} in heat-treated aragonite, American Mineralogist, 57, 1115-1124.

DISTRIBUTION LIST

DEPARTMENT OF DEFENSE

Assistant to the Secretary of Defense
Atomic Energy
ATTN: Executive Assistant

Defense Advance Rsch. Proj. Agency
ATTN: TIO

Defense Civil Preparedness Agency
ATTN: Hazard Eval & Vul Red Div, G. Sisson

Defense Documentation Center
12 cy ATTN: DD

Defense Intelligence Agency
ATTN: DB-4C, E O'Farrel
ATTN: DB-4E

Defense Nuclear Agency
2 cy ATTN: SPSS
4 cy ATTN: TITL
ATTN: DDST

Field Command Defense Nuclear Agency
ATTN: FCPR
ATTN: FCTMOF

Field Command Defense Nuclear Agency
ATTN: FCPRL

Interservice Nuclear Weapons School
ATTN: TTV

NATO SCHOOL (SHAPE)
ATTN: U.S. Documents Officer

Under Secy. of Def. for Rsch. & Engrg.
ATTN: Strategic & Space Systems (OS)

DEPARTMENT OF THE ARMY

BMD Advanced Technology Center
Department of the Army
ATTN: 1CRDABH-X
ATTN: ATC-T

Chief of Engineers
Department of the Army
ATTN: DAEN-MCE-D
ATTN: DAEN-RDM

Harry Diamond Laboratories
Department of the Army
ATTN: DELHD-I-TL
ATTN: DELHD-N-P

U.S. Army Ballistic Research Labs
ATTN: DRDAR-BLE, J. Keefer
ATTN: DRDAR-BLT, W. Taylor
ATTN: DRDAR-DSB-S

U.S. Army Engineer Center
ATTN: DT-LRC

Division Engineer
U.S. Army Engineer Division, Huntsville
ATTN: HNDED-SR

DEPARTMENT OF THE ARMY (Continued)

Division Engineer
U.S. Army Engineer Division, Ohio River
ATTN: ORDAS-L

U.S. Army Engr. Waterways Exper. Station
ATTN: J. Strange
ATTN: G. Jackson
ATTN: W. Flathau
ATTN: L. Ingram
ATTN: Library

U.S. Army Material & Mechanics Rsch. Ctr.
ATTN: Technical Library

U.S. Army Materiel Dev. & Readiness Cmd.
ATTN: DRXAM-TL

U.S. Army Missile R&D Command
ATTN: RSIC

U.S. Army Nuclear & Chemical Agency
ATTN: Library

DEPARTMENT OF THE NAVY

Civil Engineering Laboratory
Naval Construction Battalion Center
ATTN: Code L51, S. Jakahashi
ATTN: Code L51, R. Odello
ATTN: Code L08A

Naval Facilities Engineering Command
ATTN: Code 09M22C

Naval Material Command
ATTN: MAT 08T-22

Naval Postgraduate School
ATTN: Code 0142

Naval Research Laboratory
ATTN: Code 2627

Naval Surface Weapons Center
ATTN: Code F31

Naval Surface Weapons Center
ATTN: Technical Library & Information Services Branch

Naval War College
ATTN: Code E-11

Naval Weapons Evaluation Facility
ATTN: Code 10

Office of Naval Research
ATTN: Code 474, N. Perrone
ATTN: Code 715

Strategic Systems Project Office
Department of the Navy
ATTN: NSP-43

DEPARTMENT OF THE AIR FORCE

Air Force Geophysics Laboratory
ATTN: LWW, K. Thompson

Air Force Institute of Technology, Air University
ATTN: Library

Air Force Systems Command
ATTN: DLW

Air Force Weapons Laboratory
ATTN: DE, M. Plamondon
ATTN: SUL
ATTN: DES, J. Shinn
ATTN: DES, J. Thomas

Assistant Chief of Staff, Intelligence
Department of the Air Force
ATTN: INT

Deputy Chief of Staff, Research, Development, & ACQ
Department of the Air Force
ATTN: AFRDQSM

Foreign Technology Division, AFSC
Department of the Air Force
ATTN: NIIS Library

Rome Air Development Center, AFSC
Department of the Air Force
ATTN: Documents Library

Space & Missile Systems Organization
Department of the Air Force
ATTN: MNN

Strategic Air Command
ATTN: NRI-STINFO Library

DEPARTMENT OF ENERGY

Department of Energy
Albuquerque Operations Office
ATTN: Doc. Con. for Technical Library

Department of Energy
Library Room G-042
ATTN: Doc. Con. for Classified Library

Department of Energy
Nevada Operations Office
ATTN: Doc. Con. for Technical Library

DEPARTMENT OF ENERGY CONTRACTORS

Lawrence Livermore Laboratory
ATTN: Tech. Info. Dept. Library
ATTN: L-96, L. Woodruff

Los Alamos Scientific Laboratory
ATTN: Reports Library
ATTN: R. Bridwell

Oak Ridge National Laboratory
Union Carbide Corporation, Nuclear Division
X-10 Lab Records Division
ATTN: Technical Library
ATTN: Civil Def. Res. Proj.

DEPARTMENT OF ENERGY CONTRACTORS (Continued)

Sandia Laboratories
ATTN: L. Hill
ATTN: 3141
ATTN: S. Chabai

Sandia Laboratories, Livermore
ATTN: Library & Security Class. Div.

OTHER GOVERNMENT

Central Intelligence Agency
ATTN: J. Ingley

Department of the Interior
Bureau of Mines
ATTN: Technical Library

DEPARTMENT OF DEFENSE CONTRACTORS

Aerospace Corporation
ATTN: Technical Information Services

Agbabian Associates
ATTN: M. Agbabian

Applied Theory, Inc.
2 cy ATTN: J. Trulio

AVCO Research & Systems Group
ATTN: Library A830

BDM Corporation
ATTN: Corporate Library
ATTN: T. Neighbors

Boeing Company
ATTN: Aerospace Library

California Institute of Technology
ATTN: T. Aherns
ATTN: J. Vizgirda

California Research & Technology, Inc.
ATTN: D. Orphal

California Research & Technology, Inc.
ATTN: S. Shuster
ATTN: Library
ATTN: K. Kreyenhagen

Calspan Corporation
ATTN: Library

Civil/Nuclear Systems Corporation
ATTN: J. Bratton

University of Dayton
Industrial Security Super KL-505
ATTN: H. Swift

University of Colorado Seminary
Denver Research Institute
ATTN: Sec. Officer for J. Wisotski

EG&G Washington Analytical Services Center, Inc.
ATTN: Library

DEPARTMENT OF DEFENSE CONTRACTORS (Continued)

Eric H. Wang, Civil Engineering Rsch. Fac.
ATTN: N. Baum

Gard, Incorporated
ATTN: G. Neidhardt

General Electric Company-TEMPO
Center for Advanced Studies
ATTN: DASIAC

IIT Research Institute
ATTN: Documents Library
ATTN: M. Johnson
ATTN: R. Welch

University of Illinois, Consulting Services
ATTN: N. Newmark

Institute for Defense Analyses
ATTN: Classified Library

Kaman AviDyne, Division of Kaman Sciences Corp.
ATTN: E. Criscione
ATTN: Library
ATTN: N. Hobbs

Kaman Sciences Corporation
ATTN: Library

Lockheed Missiles & Space Company, Inc.
ATTN: T. Geers
ATTN: Technical Information Center

McDonnell Douglas Corporation
ATTN: R. Halprin

Merritt CASES, Inc.
ATTN: Library
ATTN: J. Merritt

Physics International Company
ATTN: F. Sauer
ATTN: L. Behrmann
ATTN: Technical Library
ATTN: E. Moore
ATTN: J. Thomsen

R&D Associates
ATTN: C. MacDonald
ATTN: J. Lewis
ATTN: R. Port
ATTN: Technical Information Center
ATTN: A. Latter

R&D Associates
ATTN: H. Cooper

DEPARTMENT OF DEFENSE CONTRACTORS (Continued)

SRI International
ATTN: B. Gasten
ATTN: G. Abrahamson
ATTN: D. Keough
ATTN: Y. Gupta

Systems, Science & Software, Incorporated
ATTN: D. Grine
ATTN: Library
ATTN: T. Riney
ATTN: T. Cherry

Systems, Science & Software, Inc.
ATTN: J. Murphy

Terra Tek, Incorporated
ATTN: S. Green
ATTN: Library
ATTN: A. Abou-Sayed

Tetra Tech, Incorporated
ATTN: Library

TRW Defense & Space Systems Group
ATTN: Technical Information Center
2 cy ATTN: P. Dai
ATTN: P. Bhutta

TRW Defense & Space Systems Group
San Bernardino Operations
ATTN: E. Wong

Vela Seismological Center
ATTN: G. Ulrich

Weidlinger Assoc., Consulting Engineers
ATTN: M. Baron
ATTN: I. Sandler

Weidlinger Assoc., Consulting Engineers
ATTN: J. Isenberg

Science Applications, Incorporated
ATTN: Technical Library

Science Applications, Incorporated
ATTN: D. Maxwell
ATTN: D. Bernstein

Southwest Research Institute
ATTN: W. Baker
ATTN: A. Wenzel